Desalination and Water Treatment
www.deswater.com
doi: 10.5004/dwt.2019.24648

167 (2019) 291–301
November

Synthesis and low concentration Cr(VI) adsorption performance of chitosan/poly(vinyl alcohol)/Fe(III)/glutaraldehyde

Yaoguo Wu[a,*], Jianghua Zhang[a], Sihai Hu[a,b], Yuanjing Zhang[a,b], Jiangwei Chan[a], Xu Xin[a]

[a]*Department of Applied Chemistry, Northwestern Polytechnical University, Xi'an 710129, China, emails: wuygal@163.com (Y.G. Wu), camel_bird@126.com (J.H. Zhang), hsh18621@163.com (S.H. Hu), 1493877017@qq.com (Y.J. Zhang), 1987539531@qq.com (J.W. Chan), 316698050@qq.com (X. Xin)*
[b]*Key Laboratory of Groundwater Contamination and Remediation, China Geological Survey and Hebei Province, Shijiazhuang 050000, China*

Received 18 February 2019; Accepted 29 June 2019

ABSTRACT

Chitosan/polyacrylamide/poly(vinyl alcohol)/Fe/glutaraldehyde (CS/PAM/PVA/Fe/GA) was reported as an adsorbent with several advantages, while some major disadvantages such as low desorption rate and poor reutilization, which formed an obstacle to its application in low-concentration Cr(VI) adsorption performance. These major disadvantages the authors speculate might be ascribed to PAM. To test the speculation correct, CS/PVA/Fe/GA was synthesized as adsorbent and then characterized using scanning electron microscopy, Fourier transform infrared spectroscopy and X-ray photoelectron spectroscopy. Low-concentration (5.0–30.0 mg L^{-1}) Cr(VI) adsorption was tested as a function of solution pH value, Cr(VI)initial concentration and adsorption time, and its primary mechanisms were explored. The results showed that, CS/PVA/Fe/GA has not only higher desorption rate and reutilization but also higher adsorption efficiency and (3.0–10.0) pH-independence compared with CS/PAM/PVA/Fe/GA; the adsorption mechanisms were also different, the complexation of the $-NH_2$ group with Fe(III) was especially included herein. The complexation, which was insensitive to pH, mainly contributed to the above advantages, proving our speculation correct. Thus, CS/PVA/Fe/GA is an alternative adsorbent to remove Cr(VI) from natural water.

Keywords: Hexavalent chromium (Cr(VI)); Synthesis; Adsorbent; Isotherms; Kinetics

1. Introduction

Hexavalent chromium (Cr(VI)) is commonly found in natural waters including surface water and groundwater [1–5], which are usually used as drinking water [6]. However, Cr(VI) is a famous potential health hazard [3]. The World Health Organization (WHO) set a stricter threshold for total chromium in drinking water of 50 μg L^{-1} [7]. To remove Cr(VI) from the water, numerous studies had been done to find the methods, and proved adsorption was one of the great potential methods [3,8–13]. Particularly, Cr(VI) usually present in natural surface water and groundwater with low concentration needs to be treated carefully [3,13]. However, few studies on these have been conducted [14–19].

Chitosan (CS) and its derivatives have been widely employed as adsorbents to remove low concentration Cr(VI) [2,3,18,20–22]. In our previous study [23], CS/polyacrylamide/poly(vinyl alcohol)/Fe/glutaraldehyde (CS/PAM//PVA/Fe/GA) copolymer has been identified as an efficient adsorbent for low-concentration Cr(VI) adsorption, and has several advantages including fast adsorption rate, high adsorption efficiency and (3.0–8.0) pH-independence, meanwhile some major disadvantages such as low desorption rate and poor reutilization. These major disadvantages had constituted

* Corresponding author.

the obstacles in its practical application, which need to be overcome to adsorb low concentration Cr(VI) and purify the relevant water. We speculate that these disadvantages might be ascribed to PAM, whose poor hydrolytic property limits the complexation of its $–NH_2$ group with Fe(III). Actually, CS and PVA are rich in the groups of $–NH_2$ and –OH [3,8,24–28], have potential for this complexation with Fe(III). So, the present work focused on preparation and performance of CS/polyacrylamide/poly(vinyl alcohol)/Fe/glutaraldehyde (CS/PVA/Fe/GA) for low-concentration Cr(VI) adsorption, with specific objective to check our speculation and find an efficient adsorbent for low-concentration Cr(VI).

2. Materials and methods

2.1. Materials

CS (75%–85% deacetylated chitin, Mn = 50–190 kDa) was purchased from Sigma-Aldrich (St. Louis, USA). PVA (Mw = 10,000–26,000 g mol^{-1}, 86%–89% hydrolysis), GA (50% GA in water), and analytical grade $K_2Cr_2O_7$, NaCl, $NaNO_3$, $NaHCO_3$, $FeCl_3·6H_2O$, H_2SO_4, H_3PO_4, HCl and NaOH were all purchased from Merck (Merck KGaA, Darmstadt, Germany). De-ionized water was used for preparation of all the solutions in the present study.

2.2. Synthesis of CS/PVA/Fe/GA

The way to synthesize CS/PVA/Fe/GA was reported in the reference [23]. Its main process is as following: 2.00 g CS was dissolved in 50 mL acetic acid (2%, v/v) and stirred for 2 h, then the CS solution was obtained in a 250 mL flask. In another flask, PVA (0.60 g) was dissolved in 30 mL de-ionized water at 70°C for 4 h until fully dissolved, and the PVA solution was obtained. The two solutions and ferric chloride (2.5 g) were put into one 250 mL flask and stirred for 5 h, 5% 10 mL GA was then added to 2 h cross-linking reaction and a cross-linked product was obtained. The product was immersed in 2.0 M NaOH solution to be molded and the objective copolymer was produced. The copolymer was washed with hydrochloric acid (three times) and then de-ionized water (three times) to remove the unreacted raw substances, respectively, and then freeze dried. The expected adsorbent CS/PVA/Fe/GA was obtained and kept in a desiccator for use.

2.3. Preparation of Cr(VI) stock and work solutions

The stock solution with 100.0 mg L^{-1} Cr(VI) was prepared by dissolving 0.2829 g $K_2Cr_2O_7$ in 1 L de-ionized water. The work solutions with different Cr(VI) concentrations were obtained by diluting the stock $K_2Cr_2O_7$ solution.

2.4. Batch adsorption test

The batch adsorption test was performed in a water bath oscillator (120 rpm) at 25°C ± 1°C. CS/PVA/Fe/GA (0.1 g) was equilibrated with 50 mL of the work solution with different concentrations of Cr(VI). The pH was adjusted using 0.1 M NaOH or HCl solution.

The amount of Cr(VI) adsorbed per unit mass of the adsorbent (q, mg/g) was calculated via Eq. (1) as follows:

$$q = \frac{\left(C_0 - C_e\right) \times V}{m} \tag{1}$$

meanwhile, the removal percentage of Cr(VI) was determined with Eq. (2):

$$\%\text{removal} = \frac{\left(C_0 - C_e\right)}{C_0} \times 100 \tag{2}$$

where C_0 and C_e are the initial and equilibrium Cr(VI) concentrations (mg L^{-1}), respectively; m is the mass (g) of the adsorbent used, V is the volume of the work solution (L).

2.5. Methods

Cr(VI) concentration was determined by UV–Vis spectrophotometer using 1,5-diphenylcarbazide after separation [24], and UV–Vis absorbance spectra were obtained by ultraviolet–visible spectrophotometer (UV–Vis Lambda 35). Fourier transform infrared spectroscopy (FTIR) spectra are characterized via double beam spectrophotometer (Bruker, model Tensor, Germany). X-ray photoelectron spectroscopy (XPS) analysis is made on an ESCALAB 250 Xi spectrometer (Thermo Scientific, USA) with an Al K_α X-ray source, operated at 10 mA and 15 kV. The surface morphologies of the adsorbents are studied using scanning electron microscopy (SEM) of a TESCAN VEGA 3 microscope with an accelerating voltage of 10 kV. The pH of the zero point charge (pH_{zpc}) was estimated by zeta potential measurements.

3. Results and discussion

3.1. Characterization

The FTIR spectra of CS, PVA and CS/PVA/Fe/GA are presented in Fig. 1, respectively. According to the literature [24,26,27], the characteristic peaks at 1,643 and 1,325 cm^{-1}, 1,163 and 897 cm^{-1}, 1,081 and 659 $cm^{-1}$are assigned to acetyl amino groups, glycosidic bonds of CS and CS crystal molecules, respectively. Both of CS and PVA have several same characteristic bands including –OH stretching vibration absorption peak at 3,700–3,000 cm^{-1}, –C–H stretching vibration absorption peaks at 2,930 and 2,879 cm^{-1}, the overlapped peaks of –C–N and –C–H absorption peaks at 1,560 and 1,315 cm^{-1}, two vibration adsorption bands at 1,200–800 cm^{-1} and 1,315 $cm^{-1}$for –C–O and –C–O–C groups, respectively. The peak of PVA crystal molecule is at 1,126 cm^{-1}.

In the spectra of CS/PVA/Fe/GA, all the characteristic bands of CS and PVA can be found, implying CS/PVA/Fe/GA retains the functional groups of its precursors and its adsorption capacity is at least not less than its precursors. Additionally, the C=O characteristic band at 1,662 cm^{-1} reveals Fe(III) oxidation hydroxyl peak. The –C=N absorption peak at 1,678 cm^{-1} takes place the $–NH_2$ absorption peak at 1,596 cm^{-1}, showing that cross-linking reaction occurred among CS, PVA and GA. The cross-linking reaction was via destroying the intramolecular and intermolecular hydrogen bonds in CS and PVA, resulting that the –OH absorption band got narrower than that for PVA or CS, benefiting its active adsorption points exposing to pollutants such as

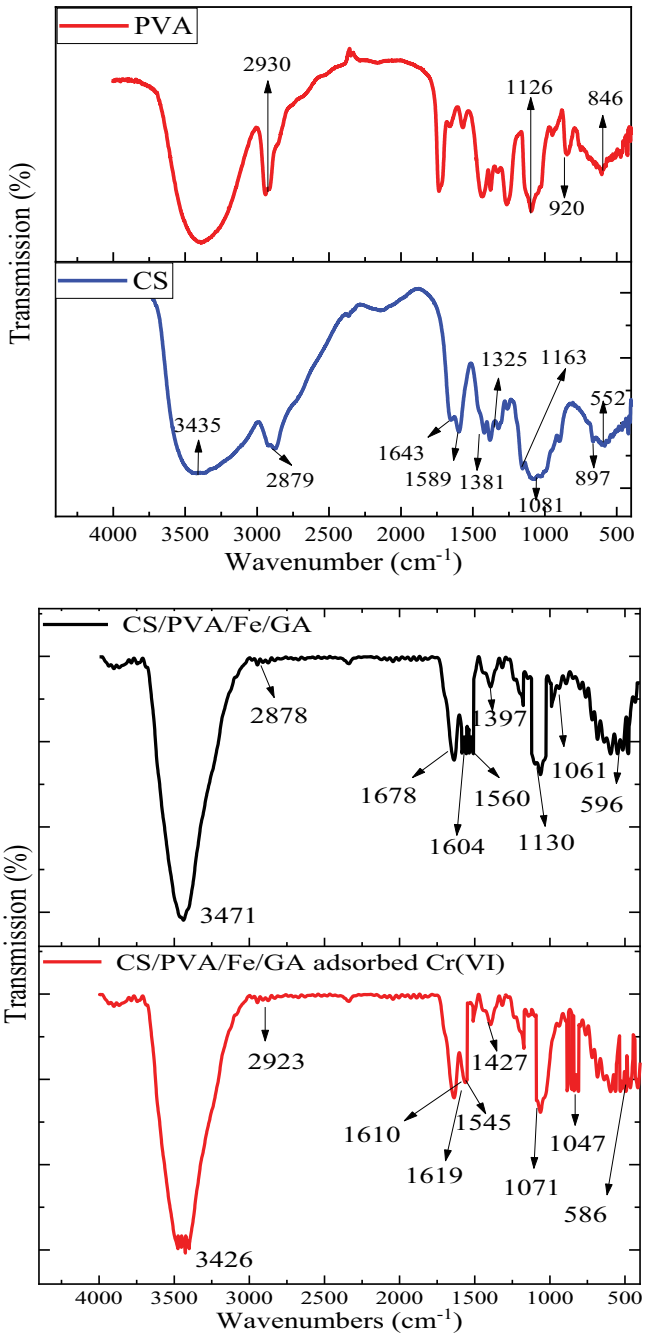

Fig. 1. FTIR spectra of PVA, CS, CS/PVA/Fe/GA and CS/PVA/Fe/GA absorbed Cr(VI).

Cr(VI). The C–OH absorption peak at 1,061 cm^{-1} for CS/PVA/Fe/GA is lower than that for CS or PVA, implying Fe(III) ion is introduced into the form of coordination [25,28–30], resulting in increasing the positive charges and enhancing the adsorption of anions including Cr(VI) on CS/PVA/Fe/GA.

Fig. 2 shows the XPS spectra of CS/PVA/Fe/GA. According to the literature [23,30], three peaks at 282.37, 283.70 and 285.81 eV in the C1s region are observed, which are consistent with C–H, C–OH and C–O–C, respectively. The binding energy peaks in the N 1s region at 397.08 and 399.25 eV, which represent –N= and N–H, was resulted from the generation of –N= functional group in the cross-linking reactions which GA participated in. Meanwhile, the group $–CONH_2$ was also converted in the cross-linking reactions, so the peaks of –O– 530 eV and O = 527 eV are observed in the O1s region. The absorption peaks of $Fe2p^{3/2}$ 710 eV and $Fe2p^{1/2}$ 725 eV proved that Fe(III) complexes with –NH and –OH [30], and –OH group was kept in CS/PVA/Fe/GA.

Fig. 3 shows SEM images of CS/PVA/Fe/GA with 2,000; 5,000; 10,000 and 20,000 magnifications, respectively. Fig. 3a shows a well-distributed porous network structure of CS/PVA/Fe/GA, and Figs. 3b–d further show that the structure is loose and the pores are non-uniform in size. These natures determine the exposure characteristics of the adsorption sites on CS/PVA/Fe/GA.

For CS/PVA/Fe/GA, the swelling ratio of was measured with mass method and is big as 640%, while its water solubility is almost negligible. The water solubility means CS/PVA/Fe/GA as adsorbent is stable in composition and structure. The big swelling ratio indicates the network structure is conducive to the solution diffusion.

All these results show CS/PVA/Fe/GA were prepared as expected, wherein the complexation reactions occurred between Fe(III) and the groups of $–NH_2$ and –OH in CS and PVA. All the characteristics of CS/PVA/Fe/GA imply that it should be one of the most promising adsorbents to remove Cr(VI) from water.

The charges of CS and CS/PVA/Fe/GA at different pH values are monitored and their results show that the points of zero charge (pH_{pzc}) of the two materials are 9.1 and 9.8, respectively. At pH < pH_{pzc}, the adsorbent surface is positively charged, thereby attracting anions and repelling cations in the solution. Because the pH_{pzc} of CS/PVA/Fe/GA is bigger than that of CS and also by far than 7.2 of CS/PAM/PVA/Fe/GA [23], the solution pH required to make the surface charge positive for CS/PVA/Fe/GA is significantly higher than that for CS. All the Cr(VI) species including hydrogen chromate ($HCrO_4^-$), dichromate ($Cr_2O_7^{2-}$) and chromate (CrO_4^{2-}) are negatively charged although effected by the solution pH [3]. Thus, CS/PVA/Fe/GA as adsorbent can be used in a pH wider range than CS and CS/PAM/PVA/Fe/GA.

3.2. *Effect of the solution pH on Cr(VI) adsorption on CS/PVA/Fe/GA*

The tests under 5.0 mg/L Cr(VI), 1.40 g/L CS/PVA/Fe/GA and 25°C ± 1°C, were performed at the initial pH values of 3.0, 5.0, 6.5, 8.0, 9.0 or 10.0, respectively, and their data after 5.0 h reaction were showed in Fig. 4.

Fig. 4 shows that the removal percentage of Cr(VI) via adsorption on CS/PVA/Fe/GA was high as more than 99%, and was hardly affected by pH varying in the range from 3.0 to 10.0. As expected, CS/PVA/Fe/GA had a much wider optimal pH range (from 3.0 to 10.0) than that of CS/PAM/PVA/Fe/GA (from 3.0 to 8.0) [23]. Meanwhile, the Cr(VI) adsorption capacity of CS/PVA/Fe/GA was also bigger than that of CS/PAM/PVA/Fe/GA. For example, the capacity was 3.0 mg/g for CS/PVA/Fe/GA and 2.5 mg/g for CS/PAM/PVA/Fe/GA [23] under their own optimum pH ranges, respectively.

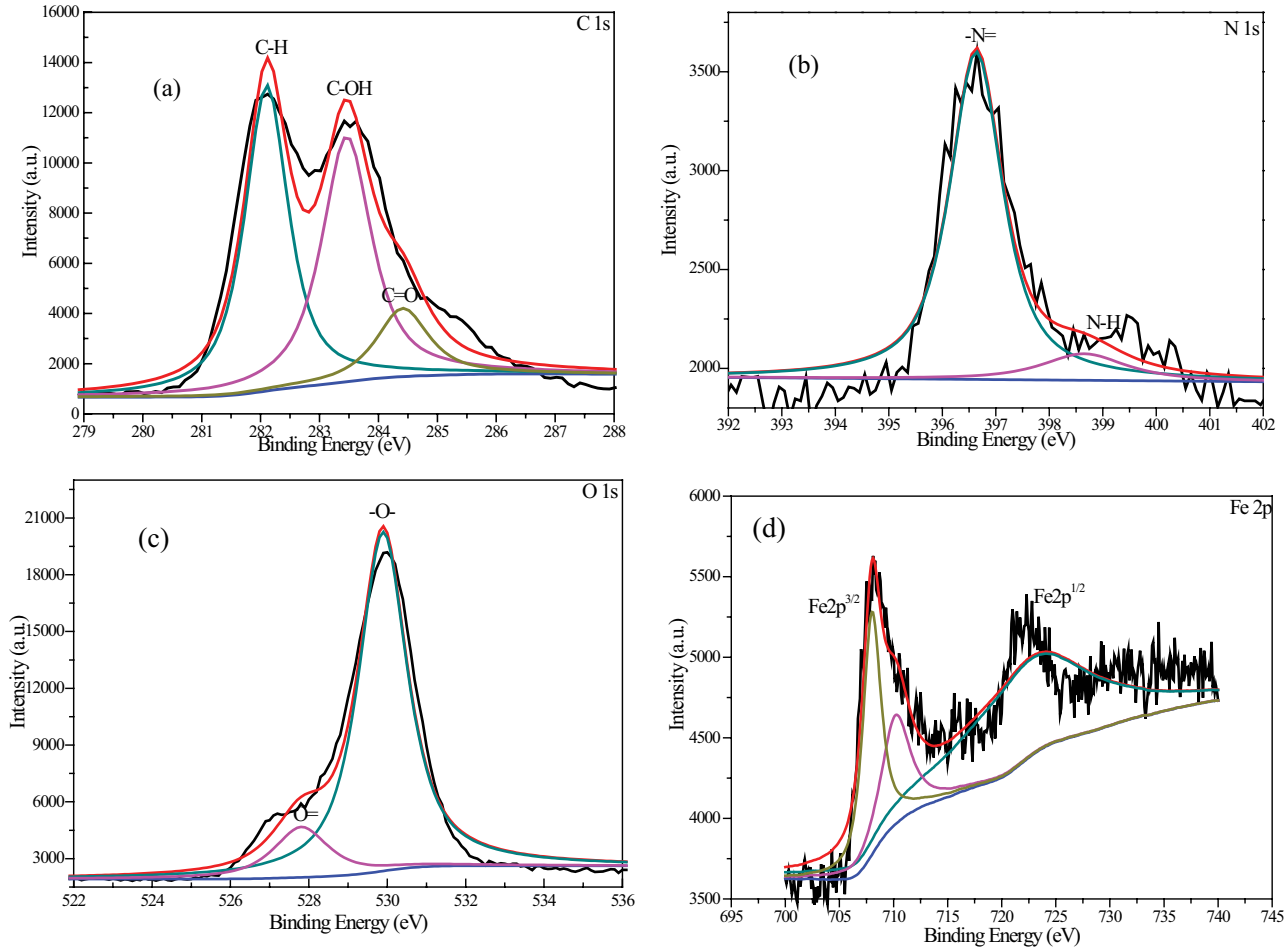

Fig. 2. XPS spectra of CS/PVA/Fe/GA.

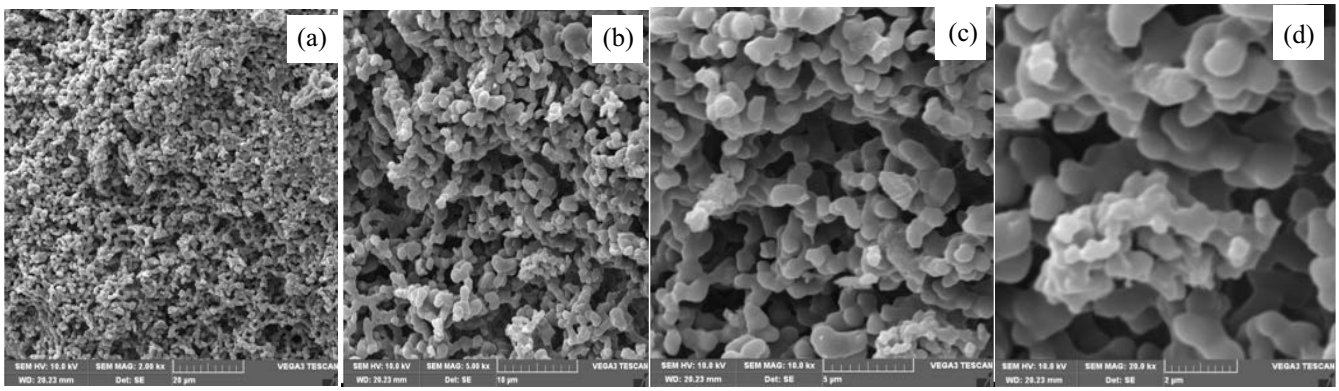

Fig. 3. SEM images of CS/PVA/Fe/GA copolymer with 2,000; 5,000; 10,000 and 20,000 magnifications.

These mentioned that CS/PVA/Fe/GA had little selectivity to Cr(VI) species including H_2CrO_4, $HCrO_4^-$, CrO_4^{2-} and $Cr_2O_7^{2-}$ which are affected by the pH value. This phenomenon might be mainly attributed to a large number of –OH and –C=N–groups in CS/PVA/Fe/GA, and the groups tend to protonate.

3.3. Effect of Cr(VI) initial concentration on Cr(VI) adsorption on CS/PVA/Fe/GA

The tests under 6.5 solution pH, 1.40 g/LCS/PVA/Fe/GA and 25°C ± 1°C, were performed at Cr(VI) initial concentrations of 5.0, 10.0, 15.0, 20.0 and 30.0 mg/L, respectively, and their data are shown in Fig. 5.

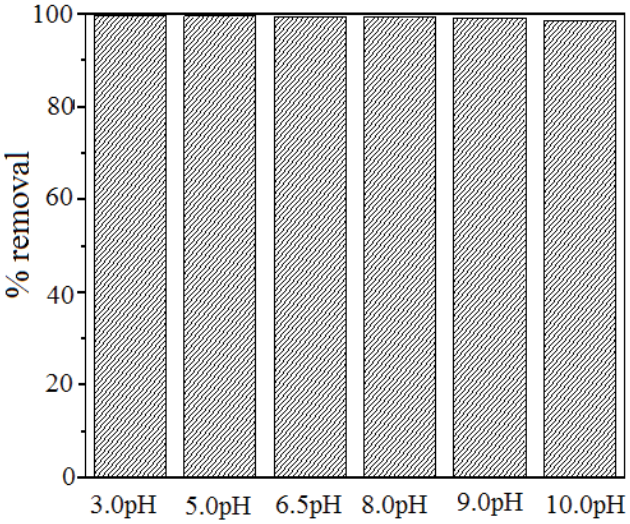

Fig. 4. Effect of the solution pH on Cr(VI) adsorption on CS/PVA/Fe/GA.

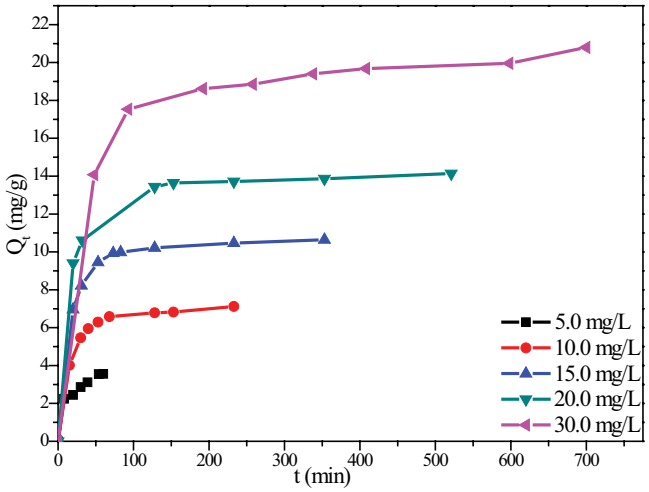

Fig. 5. Effect of Cr(VI) initial concentration on adsorption capacity on CS/PVA/Fe/GA.

From Fig. 5 it is observed that, as the initial concentration increased from 5.0 to 30.0 mg/L, the removal percentage was kept at more than 95.0%, and its equilibrium time was gotten longer from 35 to 300 min, meanwhile, the adsorption capacity of Cr(VI), Q_e, was increased from 3.5 to 19.8 mg/g. It has been reported that Cr(VI) species are also affected by its concentration, when the concentration of CrO_4^{2-} is high, chromates dimerize to form dichromate species ($H_2Cr_2O_7$ or $HCr_2O_7^-$) [31,32]. CS/PVA/Fe/GA kept its efficiency unchanged with initial concentration, showing CS/PVA/Fe/GA has little selectivity to Cr(VI) species once more. All these things were superior to that of CS/PAM/PVA/Fe/GA under the same conditions [23], implying that their adsorption mechanisms are not the same.

3.4. Effect of coexisted ions and anions

In the present study, the common anions including Cl^-, NO_3^-, $SO_4^{2-}$and HCO_3^- and the ion Cu^{2+} were selected as the co-existing species and employed to test their effects on Cr(VI) adsorption performance under 0, 0.01, 0.03 and 0.05 mol L^{-1}, respectively. Their results are presented in Fig. 6.

The results show that all the anions selected here depressed the Cr(VI) adsorption capacity (Fig. 6). The depression extents were different for each anion and ranked as HCO_3^- > SO_4^{2-} > NO_3^- > Cl^-. Nevertheless, the extent for each anion was hardly changed with its concentration, and the same phenomenon also appeared for the ion Cu^{2+}. The same order was mostly happen to CS/PAM/PVA/Fe/GA [23]. However, in the present study, the extents separated these ions and anions into two groups, HCO_3^- and the others. The effect of the latter was small and the former was great, which may be due to their similarities in molecular structure and characteristics. These showed the adsorption on CS/PVA/Fe/GA was insensitive to chemical composition except HCO_3^-. The characteristics were not found for the reported adsorbent CS/PAM/PVA/Fe/GA [23], and reveals that CS/PVA/Fe/GA is one of the best adsorbent to remove Cr(VI) from a solution

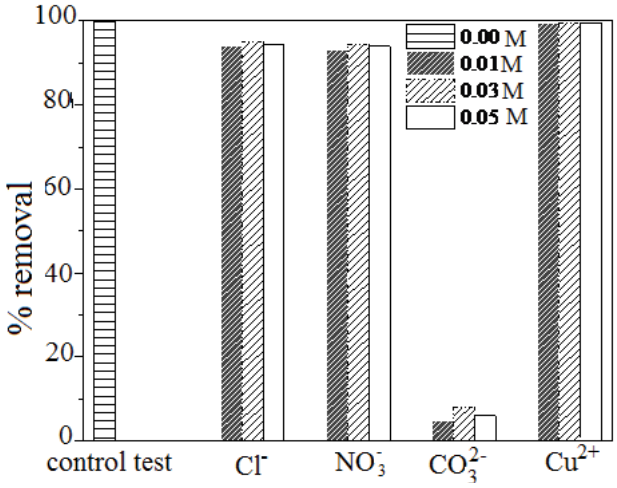

Fig. 6. Effect of coexisted ions and anions on Cr(VI) adsorption (pH = 7.0).

with low concentration of carbonate, and while a carbonate solution probably is one of the best desorption solution.

3.5. Stability and durability

With respect to the results from the effects of coexisted ions and NaOH solution used in numerous studies [17,22–23] as desorption solution for CS and its derivatives, NaOH solution and $NaHCO_3$ solution were employed in the present study and their data are shown in Figs. 7 and 8, respectively.

When 0.05 M NaOH solution was used as desorption solution, the desorption equilibrium time was about 2.0 h, the adsorption capacity remained high to 81% of the initial capacity, and the Cr(VI) equilibrium concentrations were also lower than its detected limit in the adsorption–desorption three cycles. These characteristics are superior to those of CS/PAM/PVA/Fe/GA [23], showing that CS/PVA/Fe/GA as adsorbent has high stability and durability.

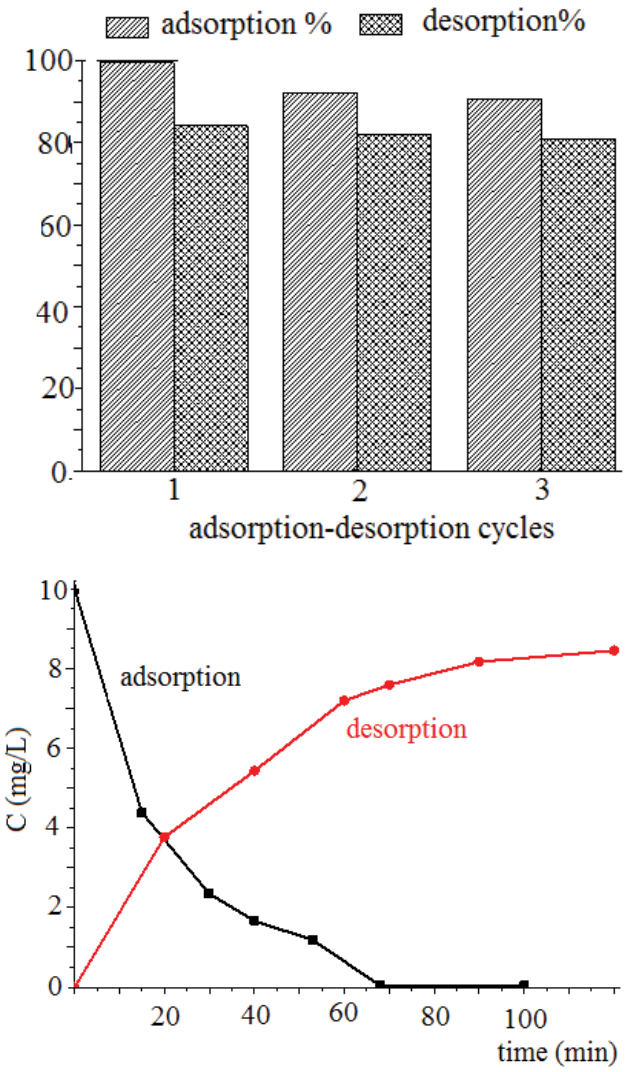

Fig. 7. Adsorption–desorption cycles study with 0.05 M NaOH solution as desorption solution.

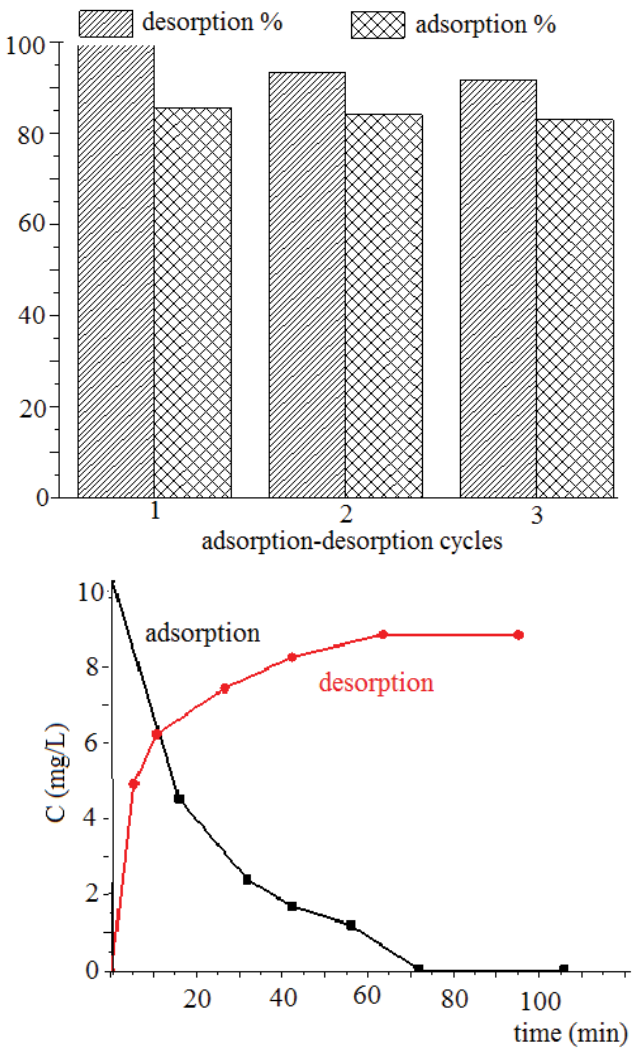

Fig. 8. Adsorption–desorption cycles study with 0.05 M $NaHCO_3$ solution as desorption solution.

When 0.05 M $NaHCO_3$ solution was used as desorption solution, compared with NaOH solution, the desorption equilibrium time was much shorter as about 1.0 h, and the adsorption capacity remained higher as more than 83% of the initial capacity, the Cr(VI) equilibrium concentrations were also lower than its detected limit in the adsorption–desorption three cycles. These showed that $NaHCO_3$ solution was more efficient than NaOH solution, and also proved CS/PVA/Fe/GA as adsorbent has high stability and durability while practicability.

3.6. Kinetics of Cr(VI) adsorption on CS/PVA/Fe/GA

The tests with 5.0, 10.0, 15.0, 20.0 or 30.0 mg L^{-1} initial concentration of Cr(VI) and 1.4 g L^{-1} CS/PVA/Fe/GA were conducted to study the kinetics of Cr(VI) adsorption, and their data are shown in Fig. 5.

The figure shows that, under these initial concentrations of Cr(VI), the adsorption equilibrium time, although increased with increasing initial concentrations of Cr(VI), was approximately 35 and 120 min at 5.0 and 20.0 mg L^{-1} initial concentrations of Cr(VI), respectively. Different equilibrium times are also reported in the literatures for the Cr(VI) adsorption on derivatives of CS, 180 min for CS at 15.0 mg L^{-1} initial concentration [33], 600 min for magnetic CS beads at 6.0 mg L^{-1} initial concentration [34], 600 min for cross-linked CS at 6.0 mg L^{-1} initial concentration [35], 180 min for Fe(III)-cross-linked CS at 5.0 mg L^{-1} initial concentration [18], and 100 min for CS/PAM/PVA/Fe/GA at 10.0 mg L^{-1} initial concentration [23]. Thus CS/PVA/Fe/GA presents a time to reach equilibrium smaller when compared with the adsorbents reported above, implying its differences with CS/PAM/PVA/Fe/GA in kinetics of Cr(VI) adsorption.

The pseudo-first-order kinetics, pseudo-second-order kinetics and intraparticle diffusion models [3,36,37] were applied to further investigate the Cr(VI) adsorption behavior on CS/PVA/Fe/GA. The first two results are shown in Table 1, and the last is presented in Fig. 9.

Table 1 shows that the R^2 value for the pseudo-second-order kinetics is bigger than that for the pseudo-first-order

Table 1
Kinetic constants of Cr(VI) absorbed on CS/PVA/Fe/GA under the studied conditions

Cr(VI)		Pseudo-first-order			Pseudo-second-order		
C_0 (mg L^{-1})	q_{exp} (mg g^{-1})	K_1	Q_e	R^2	K_2	Q_e	R^2
5.0	3.486	1.3309	3.218	0.9545	0.1860	3.503	0.9993
10.0	7.195	30.2070	6.293	0.9337	0.0082	7.015	0.9982
15.0	10.897	53.1834	11.623	0.9502	0.0074	10.923	0.9962
20.0	14.079	46.5011	13.781	0.9728	0.0059	14.186	0.9882
30.0	19.843	55.5690	17.954	0.9761	0.0047	20.806	0.9984

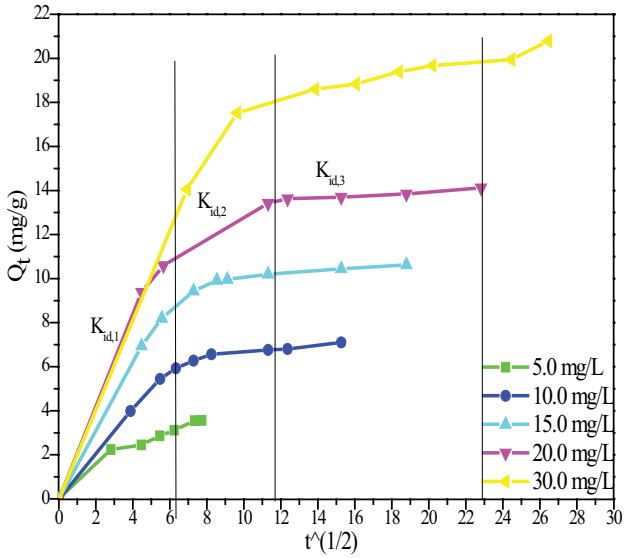

Fig. 9. Kinetic models of intraparticle diffusion at different stages (pH = 6.5, m_c = 1.4 g L^{-1}, T = 298 K).

kinetics and close to 1.0, and the maximum adsorption capacities obtained from the tests are almost equal to that from the theoretical calculation. These imply that the kinetic data were better described by the pseudo-second-order model. So, the Cr(VI) adsorption on CS/PVA/Fe/GA was due to the combined effects of chemical and physical adsorptions. However, K_2 value of the pseudo-second-order model, decreased from 0.1860 to 0.0047 with increasing Cr(VI) concentration from 5.0 to 30.0 mg L^{-1}, implying the advantages of the adsorptions preferentially occur at Cr(VI) low concentration [25,29,34], and the adsorbent is more suitable for low concentration Cr(VI) water treatment. The characteristics were also found for CS/PAM/PVA/Fe/GA [23], implying these do hardly depend on whether the absence of PMA in CS/PVA/Fe/GA and CS/PAM/PVA/Fe/GA.

Both K_{id} and C_{id}, which are the rate constants of intraparticle transport (mg g^{-1} $min^{-0.5}$) in intraparticle diffusion equation [36], can be determined via Eq. (3) based on the tests data, and their results obtained are shown in Fig. 9.

$$q_t = K_{id} t^{0.5} + C_{id} \quad (3)$$

Fig. 9 shows that the three linear portions in the plots of q_t vs. $t^{0.5}$ demonstrated the three steps of the Cr(VI) adsorption process included external surface adsorption, mesopore and micropore diffusions, respectively. Compared their slopes named $K_{id,1}$, $K_{id,2}$ and $K_{id,3}$ reflecting their corresponding adsorption rates, $K_{id,1}$ was the biggest, and the others were small and even close to zero. These denote that the adsorption process from the bulk phase to the exterior surface of the adsorbents should be the rate-controlling step but the micropore and mesopore diffusions [36]. Thus, the adsorption might be dominated mainly by electrostatic adsorption and ion exchange [11,31]. Among $K_{id,1}$, $K_{id,2}$ and $K_{id,3}$ for CS/PAM/PVA/Fe/GA were reported [23], the highest is $K_{id,2}$ and second is $K_{id,1}$, indicating that the adsorption process was ruled by mainly the mesopore diffusion and second external surface adsorption. This difference suggests that the external surface of CS/PVA/Fe/GA enabled the intradiffusion of Cr(VI). These are primarily resulted from the quantities of the positive charges and the protonated groups to adsorb Cr(VI).

3.7. Isotherms of Cr(VI) adsorption on CS/PVA/Fe/GA

Langmuir, Freundlich, Temkin and Dubinin–Radushkevich (D-R) models [31,38] were used to analyze the isotherms of Cr(VI) adsorption on CS/PVA/Fe/GA and their results are shown in Table 2.

The R^2 values reveal that Cr(VI) adsorption on CS/PVA/Fe/GA was well described by Langmuir and Temkin models. This indicates that the Cr(VI) adsorption occurs through the monolayer coverage of Cr(VI) on the surface of CS/PVA/Fe/GA, so the adsorption can be considered as the theoretical monolayer adsorption. Thus, the dimensionless separation factor (R_L) was calculated via Eq. (4) and its results were employed to evaluate favorable adsorption conditions.

$$R_L = \frac{1}{1 + K_L C_0} \quad (4)$$

where K_L is the Langmuir constant (L mg^{-1}) and C_0 is the initial Cr(VI) concentration (mg L^{-1}). A separation factor $R_L > 1$ implies unfavorable adsorption, while values ranging from 0 to 1 are indicative of a favorable adsorption process [31,39]. In this study, all the R_L values calculated for an initial concentration of 5.0, 10.0, 15.0, 20.0 and 30.0 mg L^{-1} were 0.017, 0.009, 0.006, 0.005 and 0.003, which are drawn in the range 0.003–0.017, indicating favorable Cr(VI) adsorption on CS/PVA/Fe/GA [31,39]. Temkin model shows that there was interaction of adsorbed Cr(VI) molecules on CS/PVA/Fe/GA, implying there is competition among the molecules. The R^2

Table 2
Isotherm constants for Cr(VI) adsorption (T = 298 K)

Isotherms	Parameters	
Langmuir: $q_e = \frac{Q_m K_L C_e}{1 + K_L C_e}$	Q_{max} (mg g^{-1})	22.732
	K_L (L mg^{-1})	10.970
	R^2	0.9922
Freundlich: $q_e = K_F C_e^{1/n}$	K_F (L mg^{-1})	24.599
	n	2.509
	R^2	0.9379
Temkin: $q_e = B_t \ln K_t + B_t \ln C_e$	B_t	3.982
	K_t (L mg^{-1})	76.564
	R^2	0.9870
Dubinin-Radushkevich	K_{DR} (mol^2 kJ^{-2})	0.015
$\ln q_e = \ln X_m - K_{DR}\varepsilon^2$	X_m (mg g^{-1})	16.171
	R^2	0.9711
$\varepsilon = RT \ln\left(1 + \frac{1}{C_e}\right)$	E (kJ mol^{-1})	5.882
$E = -\left(2K_{DR}\right)^{-0.5}$	q_{exp} (mg g^{-1})	20.832

value for Dubinin–Radushkevich model was lower than that for Langmuir and Temkin models, Dubinin–Radushkevich model was much less fitted with the Cr(VI) adsorption, implying that the surface of CS/PVA/Fe/GA is generally homogeneous, which is consistent with the results of SEM images above.

It was reported that Cr(VI) adsorption on CS/PAM/PVA/Fe/GA was also well fitted to Langmuir and Temkin models [14], even though, its R_L values were much bigger than that for CS/PVA/Fe/GA. This implies that Cr(VI) more tends to be adsorbed on CS/PVA/Fe/GA than CS/PAM/PVA/Fe/GA.

3.8. Proposed mechanism of Cr(VI) adsorption on CS/PVA/Fe/GA

In the batch tests above, the concentrations of Cr(VI), Cr(III) and total Cr were analyzed after their adsorption equilibrium and are shown in Fig. 10. The figure shows that both Cr(VI) and Cr(III) were found in the studied solution, revealing that Cr(VI) took part in reduction reaction and resulted in the presence of Cr(III) here.

FTIR spectra of CS/PVA/Fe/GA with adsorbed Cr(VI) are also presented in Fig. 1. Compared with CS/PVA/Fe/GA, the several characteristic absorption peaks were shifted because of the adsorption, including 2,878; 1,678; 1,560; 1,061 and 596 cm^{-1} absorption peak shifted to 2,923; 1,610; 1,545; 1,061 and 586 cm^{-1}, respectively. All these mentioned the functional groups included –C=N,–C–OH, –NH and –C–O were involved in the adsorption process.

To further clarify the roles of these functional groups in the adsorption process, XPS scan spectra of CS/PVA/Fe/GA with adsorbed Cr(VI) were analyzed and then shown in Fig. 11. It was found from Fig. 11, Cr 2p was deconvoluted into two peaks, Cr(III) at 587 eV and Cr(VI) at 576 eV [40], showing Cr(VI) was absorbed and then partly transformed into Cr(III). C 1s was deconvoluted into three peaks, C–H at 282.37 eV, C–OH$^+$–Cr at 283.70 eV and C–O–Cr at 285.81 eV. N 1s was deconvoluted into two peaks, –N=$^+$ at 397.08 eV and

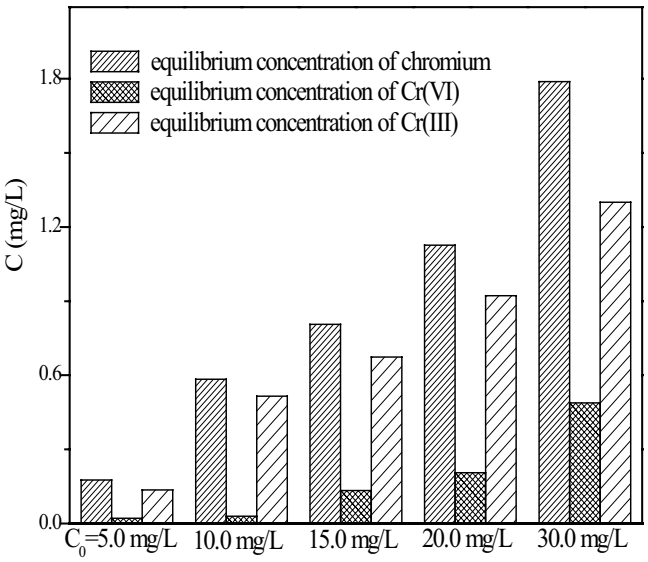

Fig. 10. Concentrations of Cr(VI), Cr(III) and total Cr in the studied solutions.

–NH at 399.25 eV. These show that Cr(VI) was absorbed by protonated groups including C–OH$^+$ and –N=$^+$ meanwhile took part in the complexation with –C–O in CS/PVA/Fe/GA [41]. For O 1s, –O– absorption peak was at 530 eV but O= absorption peak at 527 eV, showing C=O group was oxidized by Cr(VI) into C–O and resulted in Cr(III) produced [41]. The absorption peaks of Fe2p$^{3/2}$ 710 eV and Fe2p$^{1/2}$ 725 eV were observed [23,34] and proved Fe(III) presented in CS/PVA/Fe/GA. CS/PVA/Fe/GA adsorbed Cr(VI) with the groups such as C–O and Fe(III) via electrostatic interaction.

In summary, the primary mechanisms for the Cr(VI) adsorption on CS/PVA/Fe/GA covered three types of reactions, which are (1) electrostatic interaction, (2) reduction and (3) complexation, and were schematized as Fig. 12 shown. Compared with CS/PAM/PVA/Fe/GA, the role of complexation is much more important in the Cr(VI) adsorption on CS/PVA/Fe/GA, because that the majority of Fe(III) was in the complexation with –NH$_2$ in CS and PVA and decreased the oxidization C=O group in CS/PVA/Fe/GA. Although Cr(VI) species are changed with pH, their electrical property and structure remain generally unchanged. The complexation is also insensitive to pH. All these resulted in the advantages of CS/PVA/Fe/GA, and were formed in the absence of PAM, proving our speculation correct.

4. Conclusions

CS/PAM/PVA/Fe/GA was reported in our previous study as an efficient adsorbent for low-concentration Cr(VI) adsorption with low desorption rate and poor reutilization [23]. These disadvantages we speculate are due to PAM. To prove the speculation correct, CS/PVA/Fe/GA was synthesized and properties and mechanisms of its low-concentration Cr(VI) adsorption were studied with specific focus on the role of PAM here into. The results showed that, compared with CS/PAM/PVA/Fe/GA [23], CS/PVA/Fe/GA was obtained as expected, and has more positive charges and more functional groups included C–OH$^+$ and –N=$^+$ protonated groups

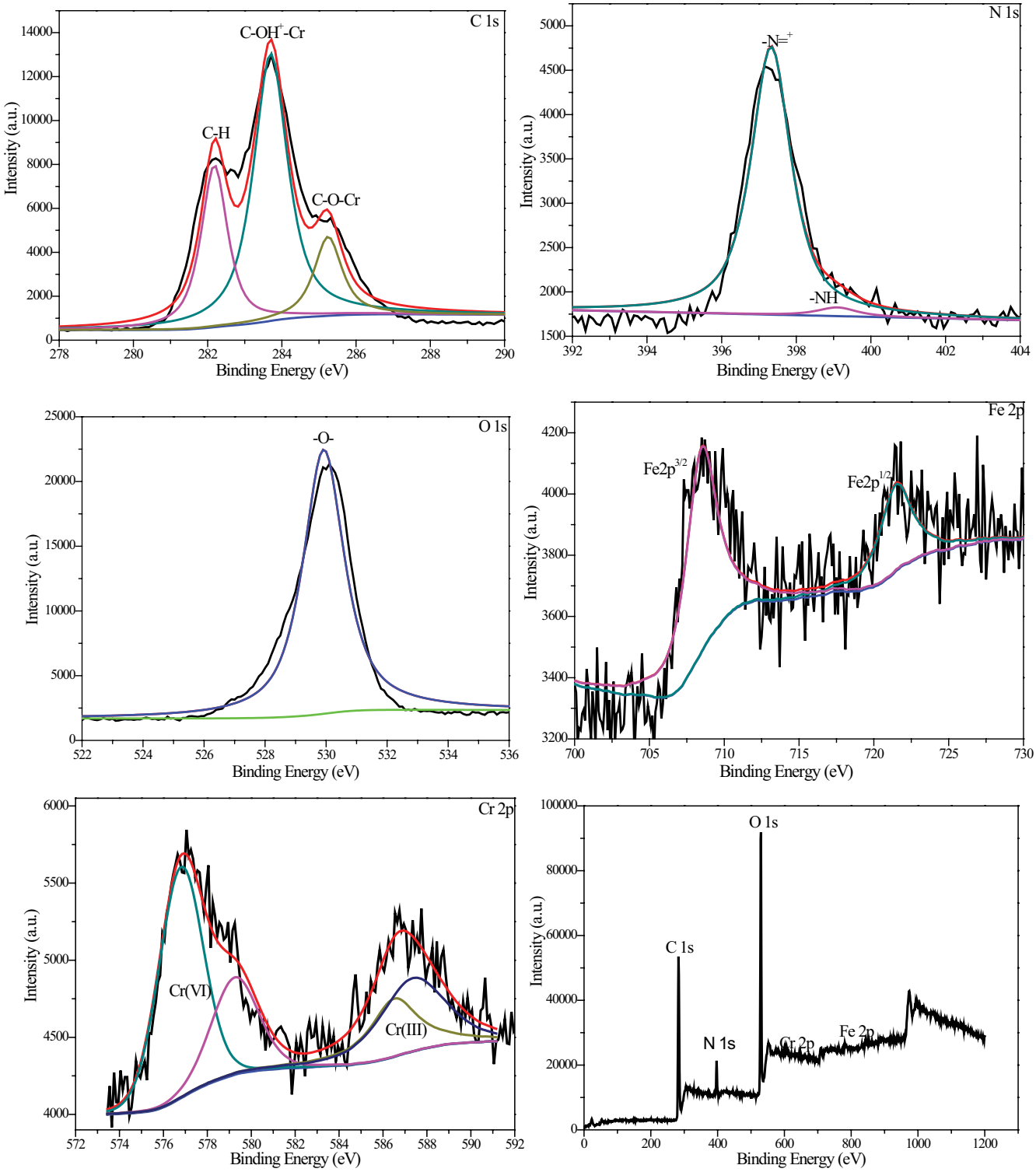

Fig. 11. XPS spectra of CS/PVA/Fe/GA with adsorbed Cr(VI).

and –C–O and –NH groups with complexing ability; CS/PVA/Fe/GA was an efficient adsorbent with more than 99% Cr(VI) adsorption percentage and was hardly affected by pH varying from 3.0 to 10.0, and a big capacity (3.0 mg g^{-1} at 5.0 mg L^{-1} Cr(VI) initial concentration). Among the studied ions included Cl^-, NO_3^-, SO_4^{2-}, HCO_3^- and Cu^{2+}, HCO_3^- had important influence on the adsorption. With 0.05 M $NaHCO_3$ or NaOH solution as desorption solution, the adsorption capacity remained as high as more than 83% of the initial capacity in the adsorption–desorption three cycles. These

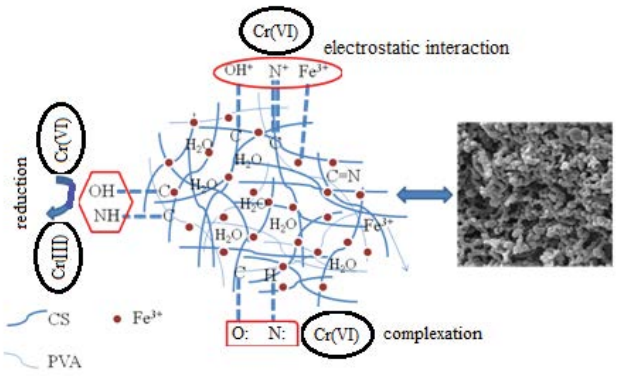

Fig. 12. Primary mechanisms of Cr(VI) adsorption on CS/PVA/Fe/GA.

characteristics were more high-quality than that of CS/PAM/PVA/Fe/GA [23]. The Cr(VI) adsorption on CS/PVA/Fe/GA well described by the pseudo-second-order kinetics, implying the combined effects of chemical and physical adsorptions and more suitable for low concentration Cr(VI). Based on intraparticle diffusion model, it was recognized that the adsorption might be dominated mainly by electrostatic adsorption and ion exchange. Langmuir and Temkin models well described the adsorption, showing theoretical monolayer adsorption and physical adsorption hereinto. Cr(VI) and Cr(III) were found in the solution and CS/PVA/Fe/GA after the adsorption equilibrium. Combined with analyzing the XPS scan spectra and FTIR spectra, the primary mechanisms for the Cr(VI) adsorption on CS/PVA/Fe/GA were referred to electrostatic interaction, reduction and complexation. The complexation was enhanced via the absence of PAM, and essential to the advantages of CS/PVA/Fe/GA. All these proved our speculation correct, and CS/PVA/Fe/GA was an efficient adsorbent for low-concentration Cr(VI) adsorption.

Disclosure statement

The authors declare no competing interests.

Funding

The authors gratefully acknowledge the financial support by National Natural Science Foundation of China (No. 41502240; No. 41601338), the Natural Science Basic Research Plan in Shaanxi Province of China (No. 2018JQ4019; No. 2017JM4005), the Fundamental Research Funds for the Central Universities (No. 3102018zy042; No. 3102017zy056), the Key Laboratory of Groundwater Contamination and Remediation, China Geological Survey (CGS) and Hebei Province (No. KF201610).

References

[1] H. Ali, E. Khan, What are heavy metals? Long-standing controversy over the scientific use of the term 'Heavy metals' – proposal of a comprehensive definition, Toxicol. Environ. Chem., 100 (2018) 6–19.
[2] M.A. Fukushima, K. Nakayasu, S. Tanaka, H. Nakamura, Speciation analysis of chromium after reduction of chromium (VI) by humic acid, Toxicol. Environ. Chem., 62 (1997) 207–215.
[3] R. Rakhunde, L. Deshpande, H.D. Juneja, Chemical speciation of chromium in water: a review, Crit. Rev. Env. Sci. Technol., 42 (2015) 776–810.
[4] Y.-g. Wu, Y.-n. Xu, J.-h. Zhang, S.-h. Hu, Evaluation of ecological risk and primary empirical research on heavy metals in polluted soil over Xiaoqinling gold mining region, Shaanxi, China, Trans. Nonferrous Met. Soc. China, 20 (2010) 688–694.
[5] J. Zhang, Y. Xu, Y. Wu, S. Hu, Y. Zhang, Dynamic characteristics of heavy metal accumulation in the farmland soil over Xiaoqinling gold-mining region, Shaanxi, China, Environ. Earth Sci., 78 (2019) 18–25.
[6] K.M. Hiscock, T. Grischek, Attenuation of groundwater pollution by bank filtration, J. Hydrol., 266 (2002) 139–144.
[7] WHO Chromium in Drinking-Water, Background Document for Preparation of WHO Guidelines for Drinking-Water Quality, World Health Organization, Geneva (WHO/SDE/WSH/03.04/4), 2003.
[8] S. Lata, P.K. Singh, S.R. Samadder, Regeneration of adsorbents and recovery of heavy metals: a review, Int. J. Environ. Sci. Technol., 12 (2015) 1461–1478.
[9] C. Lu, Y. Wu, S. Hu, Mobilization and transport of metal-rich colloidal particles from mine tailings into soil under transient chemical and physical conditions, Environ. Sci. Pollut. Res., 23 (2016) 8021–8034.
[10] C. Lu, Y. Wu, S. Hu, Drying-wetting cycles facilitated mobilization and transport of metal-rich colloidal particles from exposed mine tailing into Soil in a gold mining region along the silk road, Environ. Sci. Pollut. Res., 75 (2016) 1–12.
[11] Y. Wu, Y. Zhang, J. Qian, X. Xin, S. Hu, S. Zhang, J. Wei, An exploratory study on low-concentration hexavalent chromium adsorption by Fe(III)-cross-linked chitosan beads, R. Soc. Open Sci., 4 (2017) 170905.
[12] B. Zhou, Y. Wu, J. Chan, S. Wang, S. Hu, Batch adsorption and column transport studies of 2,4,6-trinitrotoluene in Chinese loess, Bull. Environ. Contam. Toxicol., 102 (2019) 272–278.
[13] B. Zhou, Y. Wu, J. Chan, S. Wang, S. Hu, Wetting-drying cycles enhance the release and transport of autochthonous colloidal particles in Chinese loess, Hum. Ecol. Risk Assess., 25 (2019) 1571402.
[14] M.H. Dehghani, D. Sanaei, I. Ali, A. Bhatnagar, Removal of chromium(VI) from aqueous solution using treated waste newspaper as a low-cost adsorbent: kinetic modeling and isotherm studies, J. Mol. Liq., 215 (2016) 671–679.
[15] M.H. Dehghani, A. Zarei, A. Mesdaghinia, R. Nabizadeh, M. Alimohammadi, M. Afsharnia, Adsorption of Cr(VI) ions from aqueous systems using thermally sodium organo-bentonite biopolymer composite (TSOBC): response surface methodology, isotherm, kinetic and thermodynamic studies, Desal. Wat. Treat., 85 (2017) 298–312.
[16] J. Niu, X. Jia, Y. Zhao, Y. Liu, Y. Zhong, Z. Zhai, Z. Li, Adsorbing low concentrations of Cr(VI) onto CeO_2@ZSM-5 and the adsorption kinetics, isotherms and thermodynamics, Water Sci. Technol., 77 (2018) 2327–2340.
[17] X. Sun, Z. Jing, H. Wang, J. Li, Removal of low concentration Cr(VI) from aqueous solution by modified wheat straw, J. Appl. Polym. Sci., 129 (2013) 1555–1562.
[18] N. Yi, Y. Wu, J. Wei, S. Zhang, P. Ji, Adsorption of the low concentration Cr(VI) on magnetic chitosan/PVA hydrogel beads, Fresenius Environ. Bull., 25 (2016) 2174–2182.
[19] Y. Wu, L. Fan, S. Hu, S. Wang, H. Yao, K. Wang, Role of dissolved iron ions in nanoparticulate zero-valent iron/H_2O_2 Fenton-like system, Int. J. Environ. Sci. Technol., 16 (2019) 4551–4562.
[20] A.Y. Andelib, A.N. Deveci, Adsorption of chromium on chitosan: optimization, kinetics and thermodynamics, Chem. Eng. J., 151 (2009) 188–194.
[21] V.M. Boddu, K. Abburi, J.L. Talbott, Removal of hexavalent chromium from wastewater using a new composite chitosan biosorbent, Environ. Sci. Technol., 37 (2003) 4449–4456.
[22] S. Kahu, A. Shekhawat, D. Saravanan, R. Jugade, Ionic solid-impregnated sulphate-crosslinked chitosan for effective adsorption of hexavalent chromium from effluents, Int. J. Environ. Sci. Technol., 13 (2016) 2269–2282.
[23] X. Xin, Y. Wu, S. Hu, Y. Zhang, Preparation and performance analysis of chitosan/polyacrylamide/poly (vinyl alcohol)/Fe/

glutaraldehyde copolymer for Cr(VI) adsorption, Desal. Wat. Treat., 102 (2018) 151–164.
[24] M. Amara, H. Kerdjoudj, A modified anion-exchange membrane applied to purification of effluent containing different anions pretreatment before desalination, Desalination, 206 (2007) 205–209.
[25] H. Cui, M. Fu, S. Yu, M. Wang, Reduction and removal of Cr(VI) from aqueous solutions using modified by products of beer production, J. Hazard. Mater., 186 (2011) 1625–1631.
[26] R.A.A. Muzzarelli, J. Boudrant, D. Meyer, N. Manno, M. Demarchis, M.G. Paoletti, Current views on fungal chitin/chitosan, human chitinases, food preservation, glucans, pectins and inulin: a tribute to henri braconnot, precursor of the carbohydrate polymers science, on the chitin bicentennial, Carbohydr. Polym., 87 (2012) 995–1012.
[27] M.G. Rajiv, S. Meenakshi, Preparation of amino terminated polyamidoamine functionalized chitosan beads and its Cr(VI) uptake studies, Carbohydr. Polym., 91 (2013) 631–637.
[28] T. Zhou, L. Fang, X. Wang, M. Han, S. Zhang, R. Han, Adsorption of the herbicide 2,4-dichlorophenoxyacetic acid by Fe-cross-linked chitosan complex in batch mode, Desal. Wat. Treat., 70 (2017) 294–301.
[29] N.R. Kildeeva, P.A. Perminov, L.V. Vladimirov, V.V. Novikov, S.N. Mikhailov, About mechanism of chitosan cross-linking with glutaraldehyde, Russ. J. Bioorg. Chem., 35 (2009) 360–369.
[30] D. Liu, C. Poon, K. Lu, C. He, W. Lin, Self-assembled nanoscale coordination polymers with trigger release properties for effective anticancer therapy, Nat. Commun., 5 (2014) 4182–4192.
[31] V. Dimos, K.J. Haralambous, S. Malamis, A review on the recent studies for chromium species adsorption on raw and modified natural minerals, Crit. Rev. Env. Sci. Technol., 42 (2011) 1977–2016.
[32] D.E. Kimbrough, Y. Cohen, A.M. Winer, L. Creelman, A critical assessment of chromium in the environment, Crit. Rev. Env. Sci. Technol., 29 (1999) 1–49.
[33] N.N. Thinh, P.T.B. Hanh, L.T.T. Ha, L.N. Anh, T.V. Hoang, V.D. Hoang, L.H. Dang, N.V. Khoi, T.D Lam, Magnetic chitosan nanoparticles for removal of Cr(VI) from aqueous solution, Mater. Sci. Eng., 33 (2013) 1214–1218.
[34] Y. Jiang, X. Yu, T. Luo, Y. Jia, J. Liu, X. Huang, γ-Fe_2O_3 nanoparticles encapsulated millimeter-sized magnetic chitosan beads for removal of Cr(VI) from water: thermodynamics, kinetics, regeneration, and uptake mechanisms, J. Chem. Eng. Data, 58 (2013) 3142–3149.
[35] N. Lapa, R. Barbosa, M.H. Lopes, B. Mendes, P. Abelha, I. Gulyurtlu, J.S. Oliveira, Chemical and ecotoxicological characterization of ashes obtained from sewage sludge combustion in a fluidised-bed reactor, J. Hazard. Mater., 147 (2007) 175–183.
[36] W.J. Weber, J.C. Morris, Kinetics of adsorption on carbon from solutions, J. Sanit. Eng. Div. Am. Soc. Civ. Eng., 89 (1963) 31–59.
[37] R. Khosravi, A. Azizi, R. Ghaedrahmati, V.K. Gupta, S. Agarwal, Adsorption of gold from cyanide leaching solution onto activated carbon originating from coconut shell-optimization, kinetics and equilibrium studies, J. Ind. Eng. Chem., 54 (2017) 464–471.
[38] I. Langmuir, The constitution and fundamental properties of solids and liquids, J. Am. Chem. Soc., 38 (1916) 2221–2295.
[39] L. Tofan, C. Paduraru, Sorption studies of AgI, CdII and PbII ions on sulphydryl hemp fibers, Croat. Chem. Acta, 77 (2004) 581–586.
[40] L. Sun, L. Zhang, C. Liang, Z. Yuan, Y. Zhang, W. Xu, J. Zhang, Y. Chen, Chitosan modified Fe^0 nanowires in porous anodic alumina and their application for the removal of hexavalent chromium from water, J. Mater. Chem., 21 (2011) 5877–5880.
[41] B. Jiang, J. Guo, Z. Wang, X. Zheng, J. Zheng, W. Wu, M. Wu, Q. Xue, A green approach towards simultaneous remediations of chromium(VI) and arsenic(III) in aqueous solution, Chem. Eng. J., 262 (2015) 1144–1151.